Forward peaking and thermalization in the desorption of helium

Z. W. Gortel
Department of Physics, University of Alberta, Edmonton, Alberta, Canada T6G 2J1

H. J. Kreuzer
Department of Physics, Dalhousie University, Halifax, Nova Scotia, Canada B3H 3J5

(Received 26 March 1984)

Using a master-equation approach we calculate time-of-flight spectra for helium desorbing from nichrome and graphite mediated by one-phonon processes. A complete three-dimensional theory using either bulk or surface phonons confirms that strong forward peaking results due to the lack of lateral thermalization in a rapid flash experiment.

Taborek[1] has recently published angle-dependent time-of-flight spectra for helium desorbing from helium films on nichrome after a rapid temperature flash from an initial temperature of 2.09 K to 8 K. He finds strong forward peaking of desorbed particles and a shift of the maximum in the time-of-flight spectrum to later times at angles away from the surface normal. Along with his experimental data, Taborek also presents a kinematic model that shows that his data can be taken as evidence that desorption is mediated by single-phonon absorption. We report here on detailed dynamic calculations within the cascade model of phonon-mediated desorption[2] that suggest that forward peaking is the result of a lack of thermalization of the lateral degrees of freedom in the adsorbate after a rapid temperature flash. Although we obtain desorption spectra that are very similar to those obtained by Taborek,[1] we should note that in his experiment in which more than a monolayer of helium is desorbed in one flash, forward peaking might be due to collisions in the cloud of desorbing particles, as suggested by Cowin *et al.*[3] Our calculations will make detailed predictions on the degree of forward peaking and on the shift of peak positions as a function of the temperature jump applied to induce desorption. These theoretical results might be used in future experiments to decide between the two causes of forward peaking mentioned above. The calculations are fully three-dimensional and use either bulk phonons or proper surface phonons. The starting point is a master equation[2]

$$\frac{\partial}{\partial t}n(\mathbf{k},t)=\sum_{\mathbf{k}'}[W(\mathbf{k},\mathbf{k}')n(\mathbf{k}',t)-W(\mathbf{k}',\mathbf{k})n(\mathbf{k},t)] \tag{1}$$

for the occupation functions $n(\mathbf{k},t)$ that specify the probability with which state with quantum numbers $\mathbf{k}$ is occupied by a gas particle at time t. For a free gas particle $\hbar\mathbf{k}$ is its momentum; for a particle in a highly mobile adsorbate, i.e., bound in the surface potential $V_s(\mathbf{r})$ of physisorption, $\mathbf{k}=(\mathbf{k}_{||},i)$ contains one discrete index i for its bound states and a two-dimensional wave vector $\mathbf{k}_{||}$ parallel to the surface. $W(\mathbf{k},\mathbf{k}')$ is the transition probability per unit time that a particle may undergo transitions from states $\mathbf{k}'$ to $\mathbf{k}$. They are mediated by the coupling of the adsorbate to the thermal vibrations of the solid which for weakly coupled gas-solid systems is dominated by the first derivative term $-\mathbf{u}(t)\cdot\nabla V_s(\mathbf{r})$ where $\mathbf{u}(t)$ is the amplitude of the surface vibrations.[4] For highly mobile adsorbates, such as helium their static interaction with the solid can be adequately described by a potential trough approximated by a Morse potential

$$V_s(\mathbf{r})=V_s(z)=V_0\{\exp[-2\gamma(z-z_0)]-2\exp[-\gamma(z-z_0)]\}$$

depending on the distance z from the surface only, z_0 being the distance of the minimum of the potential from the surface. In calculating the transition probabilities $W(\mathbf{k},\mathbf{k}')$ one then encounters momentum conservation in the form

$$\mathbf{k}_{||}=\mathbf{q}_{||}+\mathbf{p}_{||} \tag{2}$$

for the components parallel to the surface of the particle before ($\mathbf{q}_{||}$) and after ($\mathbf{k}_{||}$) desorption and of the absorbed phonon ($\mathbf{p}_{||}$). At this stage the theory is still essentially three-dimensional. To reduce it to one dimension one would have to show that in (2) the phonon wave vector $\mathbf{p}_{||}$ is negligible. The argument goes as follows: the parallel momentum of the adsorbed molecule is $\hbar q_{||}^{1/2}=(2mk_BT_a)^{1/2}$, where T_a is the temperature of the adsorbate. To escape from a bound state of energy $E_i=E_i+\hbar^2q_{||}^2/2m$ it must acquire, at least, an energy $|E_i|$ from a phonon. Indeed, its final energy is

$$\hbar^2(k_z^2+k_{||}^2)/2m=E_i+\hbar^2q_{||}^2/2m+h\omega\ .$$

If the desorbed particles emerge typically with an energy $\frac{3}{2}k_BT_s$, we obtain a lower bound

$$\frac{q_{||}}{p_{||}}>\frac{q_{||}}{p}c_s\left[\frac{2m}{k_B}\right]^{1/2}\frac{T_a^{1/2}}{\frac{3}{2}T_s-T_a+|E_i|/k_B}\ , \tag{3}$$

where c_s is the average sound velocity. At this stage we must know from which bound states E_i particles actually desorb into the continuum. This obviously not only depends on the availability of thermal phonons but also on the relative magnitude of the transition probabilities for bound-state–bound-state versus bound-state continuum transitions which in turn depend on the details of the dynamics as we know from the cascade model.[2] For most

systems detailed calculations suggest that, indeed, the parallel phonon momentum $\mathbf{p}_{||}$ in (2) can be dropped. This, however, is not true for the nonequilibrium situation of Taborek's experiment as he correctly observed. In any case, if $\mathbf{p}_{||}$ is negligible, then the transition probabilities factorize

$$W(k,k')=\delta_{\mathbf{k}_{||},\mathbf{k}'_{||}}W(k_z,k'_z)\ . \tag{4}$$

This reduces the theory based on (1) to the one-dimensional cascade model of Ref. 2.

We will present in this paper a comparison of time-of-flight spectra for helium desorbing from a nichrome substrate calculated in the one-dimensional approximation based on (4) and the full three-dimensional version. In the latter we use (i) a bulk Debye model for the phonons and (ii) proper surface phonons.[5] We obtain, for the number of desorbed particles registered per unit time by a detector a distance L from the surface and under an angle θ to the surface normal (details can be found in Ref. 6),

$$\frac{dN^{(1)}_{\rm reg}}{dt}=\text{const}\,t^{-5}\cos\theta\exp\left[-\frac{m}{2k_BT}\left[\frac{L}{t}\right]^2\sin^2\theta\right]$$
$$\times\sum_{j=0}^{i_0}e^{-E_j/k_BT}f_j\left[\frac{\cos\theta}{t}\right]\left[\frac{m}{2}\left[\frac{L}{t}\right]^2\cos^2\theta-E_j\right]^3\left[\exp\left\{\left[\frac{m}{2}\left[\frac{L}{t}\right]^2\cos^2\theta-E_j\right]/k_BT\right\}-1\right]^{-1}$$
$$\times\Theta\left[\hbar\omega_D+E_j-\frac{m}{2}\left[\frac{L}{t}\right]^2\cos\theta\right] \tag{5}$$

and

$$\frac{dN^{(3)}}{dt}=\text{const}\,t^{-5}\cos\theta\exp\left[-\frac{m}{2k_BT_i}\left[\frac{L}{t}\right]^2\right]$$
$$\times\sum_{j=0}^{i_0}\left[\frac{m}{2}\left[\frac{L}{t}\right]^2\cos^2\theta-E_j\right]^2f_j\left[\frac{\cos\theta}{t}\right]$$
$$\times\sum_{\sigma}\int_0^{\infty}dy\,s^{(\sigma)}(y)\int_0^{\omega_D^{(\sigma)}/\omega_D}dw\,w\exp(w\hbar\omega_D/k_BT_i)$$
$$\times[\exp(w\hbar\omega_D/k_BT_f)-1]^{-1}[a^2-b^2]^{-1/2}\Theta(a-b)\Theta(a+b)\ , \tag{6}$$

where

$$a=\frac{2m\omega_D}{\hbar c_T\gamma^2}\frac{L}{t}\sin\theta w\sqrt{y}\ ,$$
$$b=\frac{2mE_j}{\hbar^2\gamma^2}+\left[\frac{\omega_D}{c_T\gamma}\right]^2w^2y+\frac{2m\omega_D}{\hbar\gamma^2}w-\left[\frac{m}{\hbar\gamma}\frac{L}{t}\cos\theta\right]^2\ , \tag{7}$$
$$f_j\left[\frac{\cos\theta}{t}\right]=\frac{\sqrt{-E_j}}{j!\Gamma(2\sigma_0-j)}\frac{\sinh\left[\frac{2mL}{\hbar\gamma t}\cos\theta\right]\left|\Gamma\left[\sigma_0+\frac{1}{2}+i\frac{mL}{\hbar\gamma t}\cos\theta\right]\right|^2}{\cos^2(\pi\sigma_0)+\sinh^2\left[\frac{\pi mL}{\hbar\gamma t}\cos\theta\right]}\ .$$

There are i_0+1 bound states at energies E_J in the surface potential. ω_D is the Debye frequency of the solid and $\sigma_0=2mV_0/(\hbar\gamma)^2$. The spectra (5) and (6) are calculated in perturbation theory assuming that the occupation functions in the adsorbate remain Maxwell-Boltzmann during the desorption process. In (5) they have a temperature T at which the isothermal desorption experiment is done. In (6) we have assigned the initial temperature T_i to the energy distribution of the lateral degrees of freedom of the adsorbed particles, and the final "flash" temperature T_f to the phonons and to the energy distribution in the surface potential $V_s(z)$. The significance of this will be discussed below. The phonon spectrum in the three-dimensional version (6) is given by either a bulk or a surface Debye model. For the former the sum over σ runs over longitudinal and tranverse modes with (for details see Ref. 5)

$$S^{(L)}(y)=\tfrac{1}{2}(l_s^2-y)^{1/2}\Theta(l_s^2-y)\ . \tag{8}$$

$$S^{(T)}(y)=\tfrac{1}{2}y(1-y)^{-1/2}\Theta(1-y)\ , \tag{9}$$

where $l_s=c_T/c_L$ is the ratio of transverse-to-longitudinal sound velocities. Note that integrating (8) and (9) over y gives the standard weight factors $l_s^3/3$ and $\frac{2}{3}$, respectively. For the surface Debye model we have three contributions in (6), namely

$$S^{(B)}(y)=(l_s-y)^{1/2}/\{(1-2y)^2+4y[(1-y)(l_s^2-y)]^{1/2}\}\Theta(l_s^2-y)\ , \tag{10}$$

$$S^{(GR)}(y)=4y(y-l_s^2)(1-y)^{1/2}/[(1-2y)^4+16y^2(y-l_s^2)(1-y)]\Theta(y-l_s^2)\Theta(1-y)\ , \tag{11}$$

$$S^{(R)}(y)=\frac{\pi}{2}(l_R^2-l_s^2)(l_R^2-1)^{1/2}\{[(l_R^2-l_s^2)^{1/2}-(l_R^2-1)^{1/2}][(3l_R^2-2)(l_R^2-l_s^2)^{1/2}l_R^2(l_R^2-1)^{1/2}]\}\delta(y-l_R^2)\ , \tag{12}$$

where $l_R=c_T/c_R$ is a solution of

$$4\{[1-(l_s/l_R)^2](1-l_R^{-2})\}^{1/2}=(2-l_R^{-2})^2 \tag{13}$$

for the Rayleigh sound velocity c_R. The Debye cutoff frequencies $\omega_D^{(\sigma)}$ can be found in Ref. 5.

The time-of-flight spectra calculated from (5) and (6) are for the desorption of helium from a monolayer of helium adsorbed on nichrome. According to Taborek[1] the heat of adsorption is about 30 K. This fixes the value of the depth of the Morse potential at $V_0/k_B\approx 45$ K if we choose for the range of the surface Morse potential, rather arbitrarily, $\gamma^{-1}=1$ Å. The Debye temperature of nichrome we take as $T_D=500$ K. The isothermal desorption time, as calculated from (1), is then given by $t_d=t_d^0\exp(Q/k_BT)$ with $t_d^0\sim 5\times 10^{-9}$s and $Q\sim 30$ K. In Fig. 1 we present the angle-dependent time-of-flight spectra for the isothermal desorption at a temperature $T=8$ K. The maxima decrease as a function of angle θ roughly like $\cos^{1.8}\theta$, i.e., somewhat stronger than Knudsen's cosine law. In Ref. 6 we compared these microscopically calculated time-of-flight spectra with an empirical formula for the time-of-flight spectrum

$$\frac{dN}{dt}\sim(t_0/t)^4\exp[-(t_0/t)^2]\cos\theta\ .$$

This is the proper time dependence as registered in a mass spectrometer in which the detection probability is proportional to $v^{-1}=t/L$. This is somewhat misleading. We therefore prefer to compare the theoretical time-of-flight spectra with the unmodified Maxwellian time-of-flight distribution with a factor $(t_0/t)^5$. It then emerges that for isothermal desorption the spectra as calculated from either (5) and (6) are slightly narrower than a Maxwellian and their maxima are shifted marginally to earlier times. We note that the spectra in Fig. 1 are the same within the accuracy of the plot whether they are calculated (i) with the one-dimensional theory based on (5), (ii) with the three-dimensional theory based on (6) ($T_i=T_f=T$) with bulk phonons (8) and (9), or (iii) with surface phonons (10)—(12). The relative contributions of the various phonon modes are as follows: Within the bulk Debye model for the phonons 94% of the total time-of-flight spectrum is generated by the transverse modes and 6% by the longitudinal phonons. Within the surface Debye model the Rayleigh mode contributes about 64%, the generalized Rayleigh mode about 29%, and the bulklike modes add the remaining 7%. These are, indeed, the same ratios with which the various modes contribute to the desorption time according to Eq. (8) and Table I in Ref. 5 in situations where the upper frequency cutoffs can be allowed to be infinite. In this case the w integration in (6) is always limited by the two Θ functions which restrict it, for the present parameters, to a narrow range around

$$w_0\sim\frac{m}{2\hbar\omega_D}\left[\frac{L}{t}\right]^2\cos^2\theta-\frac{E_j}{\hbar\omega_D}$$

so that the y integration decouples giving the weights $s^{(\sigma)}$ of Table I in Ref. 5, and reducing (6) to (5) apart from overall factors. Also note that the ratio of the sum of the weights $s^{(\sigma)}$ in the bulk and surface Debye phonon models, respectively, just give the factor by which the desorption time calculated in the surface phonon model is shorter than that obtained in the bulk phonon model; it is, e.g., 2.31 for $l_s=0.5$. An extensive discussion can be found in Ref. 5.

We next turn to a calculation of the time-of-flight spectra for a nonequilibrium desorption experiment, taking Taborek's experiment as a first candidate, i.e., desorbing He from a nichrome substrate that was heated, within 10 ns, from an initial temperature $T_i=2$ K to a final temperature $T_f=8$ K. At the latter temperature the desorption time is $t_d\sim 6\times 10^{-7}$ s. It can be argued that in this time the lateral degrees of freedom of helium atoms moving rather freely along the surface do not thermalize so that fast (8 K) He atoms emerge predominantly in the forward direction normal to the surface. To check this idea carefully we have to go beyond the perturbation theory calculation that leads to (5) and (6) and calculate the time evolution in the adsorbate by solving the master equation (1) exactly by diagonalization. We recall that $\mathbf{k}$ labels the energy eigenstates of a helium atom in the (Morse) surface potential. Neglecting corrugation in the latter along the surface, i.e., setting $V_s(r)\equiv V_s(z)$, we can write $E_{\mathbf{k}}=E_z+E_{||}$ where $E_{||}=(\hbar k_{||})^2/2m$. Also $e_z=E_i<0$ for $i=0,1,\ldots,i_0$ for the bound states in $V_s(t)$ and $E_z=(\hbar k_z)^2/2m$ for the continuum states. To describe a desorption experiment with (1) we set $n(\mathbf{k},t)\equiv 0$ for all $\mathbf{k}$

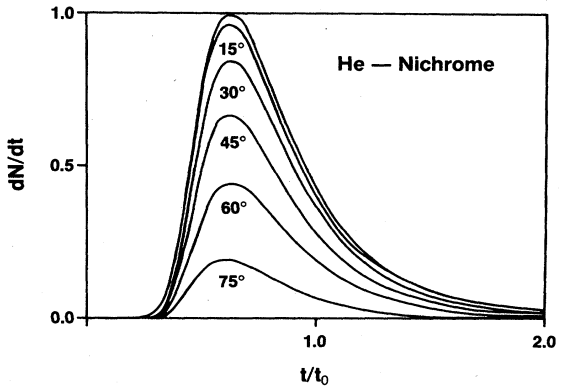

FIG. 1. Isothermal time-of-flight spectra for helium desorbing from nichrome at $T=8$ K as a function of angle θ to the surface normal. t_0 is the time needed by a thermal atom to reach the detector, $t_0=L(m/2k_BT)^{1/2}$.

with $E_z > 0$. To keep (1) as a discrete matrix equation we study a finite surface area L^2 with periodic boundary conditions so that $k_{||} = [n_x(\pi/L), n_y(\pi/L)]$ with integer n_x and n_y. The transition probabilities W in (1) and thus the distribution functions $n(\mathbf{k},t)$, of course, do not depend on the direction of $\mathbf{k}_{||}$ but only on $E_{||}$. Following a procedure outlined in Ref. 7, we coarse grain the important range of lateral energy into N discrete values $\tilde{\epsilon}_l = \tilde{\epsilon}_{\max} N^{-1}(l - \frac{1}{2})$ with $l = 1, \ldots, N$ and $\tilde{\epsilon}_{\max} = \max(\epsilon_{||})$ (all energies $\epsilon_{||}, \tilde{\epsilon}_l, \epsilon_i$, etc., are measured in units of $\hbar\omega_D$ from now on). The resulting master equation can then be written

$$\frac{d}{dt} n_i(\tilde{\epsilon}_l, t) = \sum_{i'=\rho}^{i_0} \sum_{l=0}^{N} T_{ii'}(\tilde{\epsilon}_l, \tilde{\epsilon}_{l'}) n_{i'}(\tilde{\epsilon}_{l'}, t) \ . \tag{14}$$

The transition probabilities T are given in the Appendix. They are obviously a function of the temperature T_f of the solid. Assuming that T_f can be reached from some initial temperature T_i much faster than one-phonon processes can thermalize or desorb the adsorbed helium film, we have to solve (14) with the initial conditions

$$n_i(\tilde{\epsilon}_l, t = 0) = \exp[-(\epsilon_i + \tilde{\epsilon}_l)\hbar\omega_D / k_B T_i] \ . \tag{15}$$

The solution can be written as

$$n_i(\tilde{\epsilon}_l, t) = \sum_{\kappa} S_{i\kappa} e^{-\lambda_\kappa t} \ , \tag{16}$$

where λ_κ, $\kappa = 0, 1, \ldots (i_0 + 1)N$ are real, non-negative eigenvalues of the matrix T in (14); for details see, e.g., Ref. 2. The total adsorbate coverage is given by

$$n(t) = \sum_{i,l} n_i(\tilde{\epsilon}_l, t) \ . \tag{17}$$

Let us now discuss helium desorption from a nichrome substrate that was instantly heated from $T_i = 2$ K to $T_f = 8$ K. We typically choose the cutoff energy max $(\epsilon_{||})$ for the lateral energy of the order of 10—20 K, and pick N between 50 and 100 to ensure that our coarse graining does not affect the numerical results. We note first that $\ln[n(t)]$ versus t is very linear with a slope corresponding to a desorption time $t_d = 6.25 \times 10^{-7}$ s; the linearity pertaining for $t \lesssim 5t_d$. This implies that out of the many eigenvalues λ_κ of T only the lowest one λ_0 contributes significantly in the sum (17). We note in passing that the one-dimensional version of the one-phonon theory based on (4) yields $(\lambda_0^{(1)})^{-1} = 6 \times 10^{-7}$ s. To see how much the individual occupation functions $n_i(\tilde{\epsilon}_l, t)$ change, we have plotted in Fig. 2

$$n_j(\tilde{\epsilon}_l, t) e^{\lambda_0 t} \exp\left[\left(\frac{\epsilon_j}{T_f} + \frac{\tilde{\epsilon}_l}{T_i}\right)\hbar\omega_D / k_B\right] \tag{18}$$

versus $\tilde{\epsilon}_l$ for various $\lambda_0 t$. We can infer the following: (i) from the fact that the curves for $j = 0, 1, 2$ are more or less identical we can conclude that the motion in $V_s(z)$ perpendicular to the surface thermalizes to T_f as early as $0.2 \times \lambda_0^{-1}$, i.e., with more than 80% of the adsorbate still present; (ii) the lateral motion remains characterized by the initial temperature T_i, i.e., does not thermalize even after two desorption times; (iii) the rise of all curves near the upper cutoff $\tilde{\epsilon}_{\max}$ is numerical; increasing $\tilde{\epsilon}_{\max}$ also shifts the region of upward bending to higher lateral energy $\tilde{\epsilon}_l$; (iv) the fact that for later times the slope of the curves slightly increases indicates a slow increase in temperature. This is more apparent if we plot, e.g., $\ln[n_0(\tilde{\epsilon}_l, t) e^{\lambda_0 t}]$ versus $\tilde{\epsilon}_l$ for various $\lambda_0 t$ in Fig. 3. A decreasing slope signals an increasing temperature. Also note the effect of two different cutoffs $\tilde{\epsilon}_{\max}$. From the change in slope for different $\lambda_0 t$ we can estimate the rate of lateral thermalization as 5×10^4 K s^{-1}. Performing a temperature flash from $T_i = 2$ K to $T_f = 3$ K desorbs a helium film in $t_d = 1.1 \times 10^{-3}$ s and results in a lateral heating rate of 500 K s^{-1}. Similarly for a flash from $T_i = 1$ K to $T_f = 2$ K we obtain $t_d = 0.25$ s and a lateral heating rate of about 1 K s^{-1}. Only if lateral thermalization is faster than desorption is one allowed to use thermodynamic arguments of detailed balance[8] to make statements about the desorption process. To avoid misunderstanding, we should point out that the master equation (1), of course, satisfies detailed balance in equilibrium.

We are now prepared to calculate the time-of-flight spectra for Taborek's nonequilibrium desorption experiment.[1] Indeed, we can use (6) with the distribution of lateral energies in the adsorbate kept at $T_i = 2$ K and the perpendicular motion of the surface potential thermalized to the temperature of the solid $T_f = 8$ K. The resultant Fig. 4 shows all the features of the experimental results: (i) a very strong angular dependence, and (ii) a substantial shift in the peak position to later times. For a temperature flash $T_i = 1$ K to $T_f = 2$ K less pronounced forward peaking is predicted, see Fig. 5. Because the time dependence of the theoretical time-of-flight spectra is well reproduced by a Maxwellian a very simple heuristic formula emerges for the description of a flash desorption experiment, namely

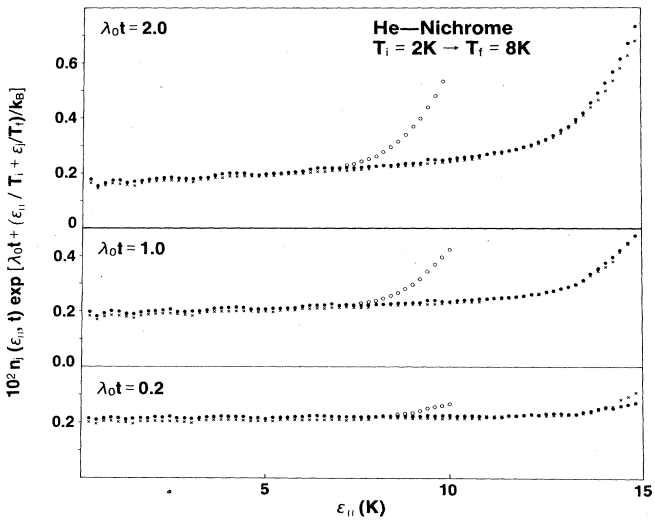

FIG. 2. Nonequilibrium distribution functions (18) for a desorption flash from $T_i = 2$ K to $T_f = 8$ K as a function of lateral energy $E_{||}$ of a Helium atom on the surface. Full points for $j = 0$; crosses for $j = 1$, open circles for $j = 0$ and a cutoff energy $E_{\max}/k_B = 10$ K. The wiggles are indicative of the numerical errors due to the coarse graining of $E_{||}$ to 75 to 50 points, respectively. λ_0^{-1} is the desorption time.

$$\frac{dN_{\rm reg}}{dt} = \text{const}\left[\frac{t_0}{t}\right]^5 \times \exp[-(t_0/t)^2(\cos^2\theta + (T_f/T_i)\sin^2\theta)]\cos\theta. \quad (19)$$

With this simple description working one is forced into the rather pessimistic conclusion that neither in isothermal nor in flash desorption experiments will time-of-flight spectra reveal significant information about the microscopic dynamics of the desorption process of He and other weakly physisorbed gases. To obtain the latter desorption times, sticking coefficients and accommodation coefficients must be measured as a function of temperature and coverage.

We can conclude this discussion by saying that forward peaking in time-of-flight desorption spectra will occur for highly mobile adsorbates if the thermalization of the lateral degrees of freedom is slow compared to the phonon-mediated desorption process. For particles heavier than helium the surface potential is more or less corrugated, leading to lateral scattering and better thermalization within the adsorbate. Collisions between particles in the adsorbate do not promote thermalization as no net energy transfer from the solid would be involved. We note, however, that scattering in the cloud of desorbed particles is argued to produce forward peaking as well.[3] Careful experiments should distinguish between these two sources of forward peaking. Our one-phonon theory makes definite predictions on the degree of forward peaking and the peak shifts as a function of the temperature jump, compare Figs. 4 and 5. As Cowin *et al.*[3] have shown, forward peaking should be reduced and eventually eliminated as the initial coverage is reduced. Our theory, of course, is applicable for small coverages. We would like to stress again that within the master-equation approach based on (1) our theory considers elementary bound-state—bound-state and bound-state—continuum transitions as mediated by the absorption or emission of one phonon at a time. The overall desorption process will, except for extremely shallow surface potentials, always involve a cascade of such one-phonon processes. The final transition from some excited bound state into the continuum, of course, involves the absorption of a last single phonon. From which of the bound states that happens depends on the particular gas-solid system. What can be said in general is that the bound-state—continuum transitions have a maximum for bound-state energies within a Debye energy $\hbar\omega_D$ from the top decaying sharply as one moves to lower bound-state energies. This implies that even in shallow surface potentials in which the ground state can be emptied by adsorbing a single phonon desorption will it still predominantly proceed from higher bound states which are, of course, replenished from the lower ones by more

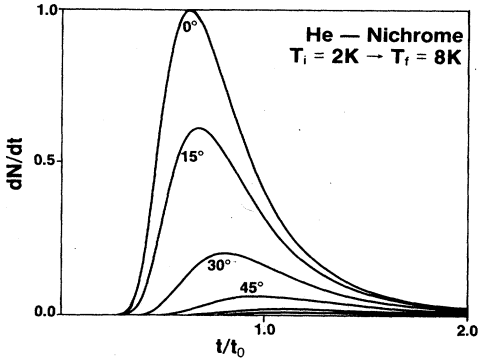

FIG. 4. Flash desorption spectra for $T_i=2$ K to $T_f=8$ K. $t_0=L(m/2k_BT_f)^{1/2}$.

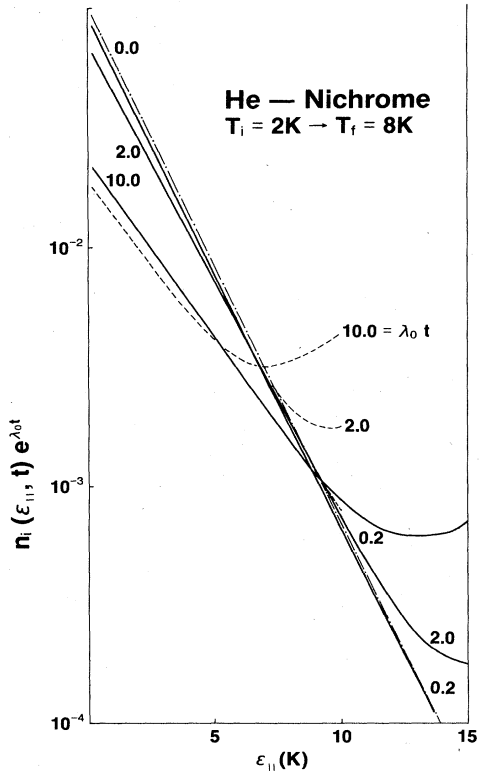

FIG. 3. Occupation functions as a function of lateral energy $E_{||}$ for various times $\lambda_0 t$. The decrease in slope reflects the heating of the lateral degrees of freedom from an initial temperature $T_i=2$ K (dashed-dotted line). The deviations from straight lines close to the upper cutoff energy ($E_{\max}/k_B=10$ K for dashed lines) reflect (i) numerical errors and (ii) nonequilibrium effects.

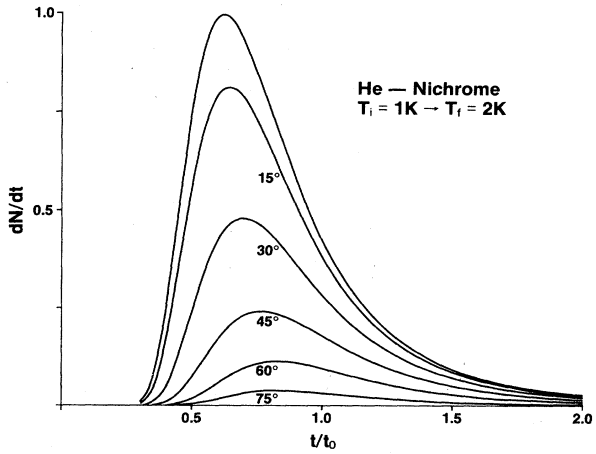

FIG. 5. Flash desorption spectra for $T_i=1$ K to $T_f=2$ K.

one-phonon absorption processes. If, e.g., in calculating the desorption time for helium desorbing from LiF (depth of the surface potential ≈ 80 K; $\hbar\omega_D = 730$ (K) one only allows desorption from the ground state the desorption times are about a factor of 4 longer than those from a proper calculation in which desorption can take place from all four bound states between which, in addition, fast bound-state–bound-state transitions maintain a quasiequilibrium. It thus seems to us somewhat artificial to try to delineate single-phonon processes from one-phonon cascades as both are based on the same transition probabilities. In this sense we would interpret the experiment by Sinvani, Taborek, and Goodstein[9] as evidence that first, i.e., after the arrival of the hot ballistic phonons, some desorption takes place at a transient high temperature established at the absorbate roughly for the duration of the phonon pulse. Because thermalization to a much lower temperature (slightly above ambient) takes place rather rapidly after the ballistic phonons are reflected the hot desorption peaks are rather small (about 5% of the total desorbed).

To see the different effects of bulk versus surface phonon modes one has to pick a gas-solid system where (i) several surface bound states are appreciably occupied, i.e., one has to work at some elevated temperature, and (ii) where the upper frequency cutoffs $\omega_p^{(\sigma)}$ in (6) are important. We look at helium desorption from a graphite surface at $T = 30$ K. The angular dependence is a bit stronger than a simple Knudsen's cosine law, something like $\cos^{1.8}\theta$. In Fig. 6 we show the time-of-flight spectra calculated from (6) with bulk phonons (dashed curve) and with surface phonons (solid curve).

Looking first at the curve calculated from the three-dimensional theory with bulk phonons, we note a small shoulder just prior to the main peak. In the one-dimensional version this structure develops into a secondary maximum followed by a discontinuous jump to the peak. Similar discontinuities develop at earlier times. To understand this feature we recall that the particles were, prior to desorption, in any one of the bound states (of energy $E_i < 0$) of the surface potential V_s. Because theory assumes that one-phonon processes are dominant the maximum kinetic energy of a particle emerging from E_i is

$$\frac{m}{2}v^2 = E_i + \hbar\omega_D \ . \tag{20}$$

Thus particles from E_i arrive at times

$$t > L\,[2(E_i + \hbar\omega_D)/m\,]^{-1/2} \ , \tag{21}$$

or with $t_0 = L(m/2k_BT)^{1/2}$,

$$\tau = \frac{t}{t_0} > [k_BT/(\hbar\omega_D + E_i)]^{1/2} \ . \tag{22}$$

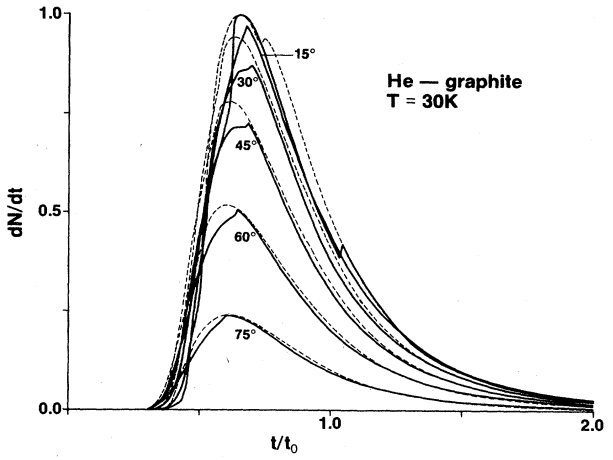

FIG. 6. Isothermal desorption spectra at $T = 30$ K. Solid curves: surface phonons; dashed curves: bulk phonons.

In a Morse potential the bound states are given by

$$\epsilon_i = \frac{E_i}{\hbar\omega_D} = -\frac{1}{r}(\sigma_0 - i - \tfrac{1}{2})^2 \ ,$$
$$\sigma_0^2 = 2mV_0/(\hbar\gamma)^2, \quad r = 2m\omega_D/\hbar\gamma^2 \ . \tag{23}$$

With the potential parameters for the helium-graphite system $\sigma_0 = 4.88$, $r = 27.46$, we find that particles will emerge from the deepest bound state $\epsilon_0 = -0.699$ for $\tau > 0.576$, from $\epsilon_1 = -0.4164$ for $\tau > 0.414$, from $\epsilon_2 = -0.2066$ for $\tau > 0.355$, from $\epsilon_3 = -0.0695$ for $\tau > 0.329$, and from $\epsilon_4 = -0.0053$ for $\tau > 0.317$. These jump discontinuities are washed out in the three-dimensional theory with bulk phonons as a result of the two integrals in (6) that average over the initial lateral momentum of adsorbed particles and phonons. If, however, we use proper surface phonons in the three-dimensional theory these discontinuities appear again whenever the Rayleigh phonons set in at times given by (20) with ω_D replaced by $\omega_D^{(R)}$ which for $l_s = c_T/c_L = 0.5$ is $\omega_D^{(R)} = 0.756\omega_D$. On smooth surfaces where surface modes can develop and can be described by elasticity theory of a semi-infinite continuum, such spectra should be observable. If the surface, however, is not smooth one could expect a depression of surface phonons so that desorption is basically triggered by bulklike phonons with bulk phonons (dashed curve).

This work was supported in part by a grant from the National Sciences and Engineering Council of Canada. We would like to thank R. Teshima for writing the computer codes. One of us (H.J.K.) would like to thank D. Goodstein for stimulating discussions on the subject.

APPENDIX

We give the matrix of transition probabilities in the master equation in (14)

$$\frac{dn_i(\tilde{\epsilon}_l)}{dt} = \sum_{i'=0}^{i_0}\sum_{l=1}^{N} T_{ii'}(\tilde{\epsilon}_l, \tilde{\epsilon}_{l'})\, n_{i'}(\tilde{\epsilon}_{l'}) \ ,$$
$$T_{ii'}(\tilde{\epsilon}_l, \tilde{\epsilon}_{l'}) = \frac{\tilde{\epsilon}_{\max}}{N}\left[M_{ii'}(\tilde{\epsilon}_l, \tilde{\epsilon}_{l'}) - \sum_{l''=1}^{N}\left[\sum_{i''=0}^{i_0} M_{i''i}(\tilde{\epsilon}_{l''}, \tilde{\epsilon}_l) + R_i(\tilde{\epsilon}_{i''}, \tilde{\epsilon}_l)\right]\delta_{ii'}\delta_{ll'}\right] \ , \tag{A1}$$

with

$$M_{ii'}(\tilde{\epsilon}_l,\tilde{\epsilon}_{l'})=M_{ii'}^{(\mathrm{abs})}(\tilde{\epsilon}_l,\tilde{\epsilon}_{l'})+M_{ii'}^{(\mathrm{em})}(\tilde{\epsilon}_l,\epsilon_{l'}) , \tag{A2}$$

$$R_i(\tilde{\epsilon}_{l'},\tilde{\epsilon}_l)=R_i^{(\mathrm{abs})}(\tilde{\epsilon}_{l'},\tilde{\epsilon}_l)+R_i^{(\mathrm{em})}(\tilde{\epsilon}_{l'},\tilde{\epsilon}_l) , \tag{A3}$$

$$M_{ii'}^{(\mathrm{abs})}(\tilde{\epsilon}_l,\tilde{\epsilon}_{l'})=\Theta(1-(\epsilon_i-\epsilon_{i'}+\tilde{\epsilon}_l-\tilde{\epsilon}_{l'}))\Theta(\epsilon_i-\epsilon_{i'}+\tilde{\epsilon}_l-\tilde{\epsilon}_{l'})(\epsilon_i-\epsilon_{i'}+\tilde{\epsilon}_l-\tilde{\epsilon}_{l'})n(\epsilon_i-\epsilon_{i'}+\tilde{\epsilon}_l-\tilde{\epsilon}_{l'})H_{ii'}G_{ii'}(\tilde{\epsilon}_l\tilde{\epsilon}_{l'}) , \tag{A4}$$

$$M_{ii'}^{(\mathrm{em})}(\tilde{\epsilon}_l,\tilde{\epsilon}_{l'})=\Theta(1-(\epsilon_{i'}-\epsilon_i+\tilde{\epsilon}_{l'}-\tilde{\epsilon}_l))\Theta(\epsilon_{i'}-\epsilon_i+\tilde{\epsilon}_{l'}-\tilde{\epsilon}_l)(\epsilon_{i'}-\epsilon_i+\tilde{\epsilon}_{l'}-\tilde{\epsilon}_l)[n(\epsilon_{i'}-\epsilon_i+\tilde{\epsilon}_{l'}-\tilde{\epsilon}_l)+1]H_{ii'}G_{ii'}(\tilde{\epsilon}_l\tilde{\epsilon}_{l'}) , \tag{A5}$$

$$H_{ii'}=6\omega_D\frac{m}{M_s}(\epsilon_i\epsilon_{i'})^{1/2}(\epsilon_i-\epsilon_i)^2\frac{i_>!\Gamma(2\sigma_0-i_>)}{i_<!\Gamma(2\sigma_0-i_<)} , \tag{A6}$$

$$G_{ii'}(\tilde{\epsilon}_l,\tilde{\epsilon}_{l'})=\tfrac{1}{2}\int_0^1 dy(1-y)^{-1/2}\frac{\Theta\left[\left[\frac{4d^2}{r}y\tilde{\epsilon}_l(\epsilon_i-\epsilon_{i'}+\tilde{\epsilon}_l-\tilde{\epsilon}_{l'})^2-\left[\tilde{\epsilon}_{l'}-\tilde{\epsilon}_l-\frac{d^2}{r}(\epsilon_i-\epsilon_{i'}+\tilde{\epsilon}_l-\tilde{\epsilon}_{l'})^2y\right]^2\right]\right]}{\left\{\left[\frac{4d^2}{r}y\tilde{\epsilon}_l(\epsilon_i-\epsilon_{i'}+\tilde{\epsilon}_l-\tilde{\epsilon}_{l'})^2-\left[\tilde{\epsilon}_{l'}-\tilde{\epsilon}_l-\frac{d^2}{r}(\epsilon_i-\epsilon_{i'}+\tilde{\epsilon}_l-\tilde{\epsilon}_{l'})^2y\right]^2\right]^{1/2}\right\}^{1/2}} , \tag{A7}$$

$$n(x)=[\exp(x\hbar\omega_D/k_BT_f)-1]^{-1} ,$$

$$R_j^{(\mathrm{abs})}(\tilde{\epsilon}_{l'},\tilde{\epsilon}_l)=\tfrac{3}{2}\omega_D\frac{m}{M_s}\frac{\sqrt{-r\epsilon_j}}{j!\Gamma(2\sigma_0-j)}$$
$$\times\int_0^1 dw\,\Theta(w+\epsilon_j+\tilde{\epsilon}_l-\tilde{\epsilon}_{l'})\frac{\sinh\{2\pi[r(w+\epsilon_j+\tilde{\epsilon}_l-\tilde{\epsilon}_{l'})]^{1/2}\}}{\cos^2(\pi\sigma_0)+\sinh^2\{\pi[r(w+\epsilon_j+\tilde{\epsilon}_l-\tilde{\epsilon}_{l'})]^{1/2}\}}$$
$$\times|\Gamma\{\sigma_0+\tfrac{1}{2}+i[r(w+\epsilon_j+\tilde{\epsilon}_l-\tilde{\epsilon}_{l'})]\}|^2(w+\tilde{\epsilon}_l-\tilde{\epsilon}_{l'})^2wn(w)G_j(w;\tilde{\epsilon}_{l'},\tilde{\epsilon}_l) , \tag{A9}$$

$$R_j^{(\mathrm{em})}(\tilde{\epsilon}_{l'},\tilde{\epsilon}_l)=\tfrac{3}{2}\omega_D\frac{m}{M_s}\frac{\sqrt{-r\epsilon_j}}{j!\Gamma(2\sigma_0-j)}$$
$$\times\int_0^1 dw\,\Theta(w+\epsilon_j+\tilde{\epsilon}_l-\tilde{\epsilon}_{l'})\frac{\sinh\{2\pi[r(w+\epsilon_j+\tilde{\epsilon}_l-\tilde{\epsilon}_{l'})]^{1/2}\}}{\cos^2(\pi\sigma_0)+\sinh^2\{\pi[r(-w+\epsilon_j+\tilde{\epsilon}_l-\tilde{\epsilon}_{l'})]^{1/2}\}}$$
$$\times|\Gamma\{\sigma_0+\tfrac{1}{2}+i[r(-w+\epsilon_j+\tilde{\epsilon}_l-\tilde{\epsilon}_{l'})]\}^{1/2}|^2(-w+\tilde{\epsilon}_l-\tilde{\epsilon}_{l'})w(n(w)+1)G_j(w;\tilde{\epsilon}_{l'},\tilde{\epsilon}_l) , \tag{A10}$$

$$G(w;\tilde{\epsilon}_{l'},\tilde{\epsilon}_l)=\tfrac{1}{2}\int_0^1 dy(1-y)^{-1/2}\frac{\Theta\left[\frac{4d^2}{r}y\tilde{\epsilon}_{l'}w^2-\left[\epsilon_l-\tilde{\epsilon}_{l'}-\frac{d^2}{r}w^2y\right]^2\right]}{\left[\frac{4d^2}{r}y\tilde{\epsilon}_{l'}w^2-\left[\tilde{\epsilon}_l-\tilde{\epsilon}_{l'}-\frac{d^2}{r}w^2y\right]^2\right]^{1/2}} . \tag{A11}$$

All energies ϵ_i and $\tilde{\epsilon}_l$ are measured in units of $\hbar\omega_D$. The calculations based on (14) leading to Figs. 2 and 3 were performed using a bulk Debye model for phonons characterized by the average Debye frequency ω_D and the average sound velocity $c_s=(M_s\omega_D/6\pi^2\rho)^{1/3}$.

The parameters for the He-nichrome system are

$$\sigma_0^2=2mV_0/(\hbar\gamma)^2=7.47 ,$$

$$r=2m\omega_D/\hbar\gamma^2=83 ,$$

$$d=\gamma c_s/\omega_D=1.728 ,$$

corresponding to ω_D, γ^{-1} and V_0 given below Eq. (13) and $c_s=1.13\times10^4$ m/s. M_s and ρ are the mass of the unit cell and the mass density of the solid, respectively, whereas $i_>/i_<$ in (46) denote larger and/or smaller value in the pair i,i'.

[1]P. Taborek, Phys. Rev. Lett. **48**, 1737 (1982).
[2]Z. W. Gortel, H. J. Kreuzer, and R. Teshima, Phys. Rev. B **22**, 5655 (1980).
[3]J. P. Cowin, D. J. Auerbach, C. Becker, and L. Wharton, Surf. Sci. **78**, 545 (1978).
[4]For the present system corrections to the dynamical coupling, due to M. W. Cole and F. Toigo, Surf. Sci. **119**, L346 (1982), are very small, as can be seen in calculations of the desorption

time by Z. W. Gortel, H. J. Kreuzer, and E. Sommer, Surf. Sci. **133**, L481 (1983).
[5]E. Goldys, Z. W. Gortel, and H. J. Kreuzer, Surf. Sci. **116**, 33 (1982).
[6]Z. W. Gortel, H. J. Kreuzer, M. Schäff, and G. Wedler, Surf. Sci. B **4**, 577 (1983).
[7]Z. W. Gortel and H. J. Kreuzer, Sur. Sci. **133**, 484 (1983).
[8]M. Weimer and D. Goodstein, Phys. Rev. Lett. **50**, 193 (1983); D. Goodstein and M. Weimer, Surf. Sci. **125**, 227 (1983); D. Goodstein, in *Many-Body Phenomena at Surfaces,* edited by D. C. Langreth and H. Suhl (to be published).
[9]M. Sinvani, P. Taborek, and D. Goodstein, Phys. Lett. **95A**, 59 (1983).